Articles

Ambipolar Organic Thin Film Transistor-like Behavior of Cationic and Anionic Phthalocyanines Fabricated Using Layer-by-Layer Deposition from Aqueous Solution

Jason Locklin,[†,‡] Kazunari Shinbo,[§] Ken Onishi,[†] Futao Kaneko,[§] Zhenan Bao,*[,||] and Rigoberto C. Advincula*[,‡]

Department of Chemistry, University of Alabama at Birmingham, Birmingham, Alabama 35294-1240, Department of Chemistry, University of Houston, Houston, Texas 77204, Department of Electrical and Electronic Engineering, Niigata University, Ikarashi 2-8050, Niigata 950-2181, Japan, and Bell Laboratories, Lucent Technologies, 600 Mountain Avenue, Murray Hill, New Jersey 07974

Received November 5, 2002. Revised Manuscript Received February 5, 2003

Organic thin film field effect transistors of water-soluble cationic and anionic phthalocyanine derivatives were successfully prepared using the layer-by-layer deposition technique. The alternating film growth and subsequent transistor properties were studied with a variety of techniques including ellipsometry, UV−vis spectroscopy, polarized UV−vis spectroscopy, AFM, and field effect transistor measurements. A stepwise and regular deposition of copper(II) phthalocyanine tetrakis(methyl pyridinium) chloride and copper(II) phthalocyanine tetrasulfonic acid, tetrasodium salt multilayers in both pure water and 0.03 M NaCl solution was observed. Differences in linear growth were observed between pure water and 0.03 M NaCl-based solutions. Polarized UV−vis spectra indicated that the conjugated phthalocyanine ring lies almost flat on the substrate surface with a random orientation within the plane of the substrate. Unusual "ambipolar" transistor-like behavior was found for the films that can be attributed to an ion-modulated electrical conduction mechanism, which relies on the assistance of mobile ions to stabilize the oxidized or reduced species in the channel region.

Introduction

There is an increasing amount of interest in the literature involving the use of conjugated polymers and oligomers as the active organic semiconductor layer in thin film devices such as light-emitting diodes (OLEDs), field effect transistors (FETs), and photovoltaic devices.[1] These materials provide certain advantages over their inorganic counterparts such as easy processing and compatibility with plastic substrates.[2] In these devices, it is crucial that the organic molecules be arranged in specific molecular architectures, where the spacing between the molecules and their orientation helps to control macroscopic properties of the material and device performance.[3] Phthalocyanines are excellent candidates for usable architectures because of their inherent symmetry, which makes rational design of supramolecular structure easier to achieve. They have shown promise as the functional component of both p- and n-channel FETs,[4] gas sensors,[5] and photovoltaic devices.[6]

* Corresponding authors. E-mail: radvincula@uh.edu (R. Advincula); zbao@lucent.com (Z. Bao).
† University of Alabama at Birmingham.
‡ University of Houston.
§ Niigata University.
|| Lucent Technologies.

(1) (a) Sheats, J. R.; Antoniadis, H.; Huescen, M.; Leonard, W.; Miller, J.; Moon, R.; Roitman, D.; Stocking, A. *Science* **1996**, *273*, 884. (b) Greenham, N. C.; Friend, R. H. *Solid State Phys.* **1996**, *49*, 21. (c) Burroughes, J. H.; Bradley, D. D. C.; Brown, A. R.; Marks, R. N.; Mackay, K.; Friend, R. H.; Burn, P. L.; Holmes, A. B. *Nature* **1990**, *347*, 539. (d) Horowitz, G. *Adv. Mater.* **1998**, *10*, 365. (e) Shaheen, S. E.; Brabec, C. J.; Sariciftci, N. S.; Padinger, F.; Fromherz, T.; Hummelen, J. C. *Appl. Phys. Lett.* **2001**, *78*, 841.

(2) (a) Bao, Z.; Rogers, J. A.; Katz, H. E. *J. Mater. Chem.* **1999**, *9*, 1895. (b) Rogers, J. A.; Bao, Z.; Baldwin, K.; Dodabalapur, A.; Crone, B.; Raju, V. R.; Kuck, V. Katz, H. Amundson, K. Ewing, J.; Drzaic, P. *Proc. Natl. Acad. Sci. U.S.A.* **2001**, *98 (9)*, 4835.

(3) (a) Tredgold, R. H. *Order in Thin Organic Films*; Cambridge University Press: Cambridge, 1994. (b) Ulman, A. *Organic Thin Films and Surfaces: Directions for the Nineties*; Academic Press: New York, 1995.

(4) (a) Guillaud, G.; Madru, M.; Al Sadoun, M.; Maitrot, M. *J. Appl. Phys.* **1989**, *166*, 4554. (b) Guillaud, G.; Al Sadoun, M.; Maitrot, M.; Simon, J.; Boubet, M. *Chem. Phys. Lett.* **1990**, *167*, 503. (c) Madru, R.; Gulliaud, G.; Al Sadoun, M.; Maitrot, M. *Chem. Phys. Lett.* **1987**, *142*, 103. (d) Madru, R.; Gulliaud, G.; Al Sadoun, M.; Maitrot, M.; Andre, J.-J.; Simon, J.; Even, R. *Chem. Phys. Lett.* **1988**, *145*, 343. (e) Bao, Z.; Lovinger, A. J.; Dodabalapur, A. *Appl. Phys. Lett.* **1996**, *69*, 3066. (f) Bao, Z.; Lovinger, A. J.; Dodabalapur, A. *Adv. Mater.* **1997**, *9*, 42. (g) Bao, Z.; Lovinger, A. J.; Brown, J. *J. Am. Chem. Soc.* **1998**, *120* (1), 207.

(5) (a) Choi, C.-G.; Lee, S.; Lee, W.-J. *Sensors Actuators, B* **1996**, *32*, 77. (b) Ding, X.; Xu, H. *Sensors Actuators, B* **2000,** *65*, 108.

(6) (a) Leznoff, C. C.; Lever, A. B. *Phthalocyanines: Properties and Applications*; VCH Publishers: New York, 1989. (b) McKeown, N. *Phthalocyanine Materials: Synthesis, structure and function*; Cambridge University Press: Cambridge, 1998.

10.1021/cm021073f CCC: $25.00
Published on Web 03/15/2003

Many techniques have been developed to assemble phthalocyanines and other organic semiconductors as thin films but the layer-by-layer control of composition and thickness is still a challenge. Thermal evaporation is the most widely used technique but this is limited to volatile, thermally durable materials. It also has its disadvantages in terms of economic feasibility for device fabrication at the industrial scale. If organic semiconductors are going to compete with their inorganic counterparts, low-cost technologies such as solution deposition or printing techniques offer the greatest advantages.

Even though solution deposition is very desirable, it has proven difficult for organic semiconductors in the past. The most common oligomeric semiconductors, such as pentacene and sexithiophene, are practically insoluble in any organic solvent. Generally, the solubility of a material can be improved through chemical structure modification, but this usually comes at the cost of device performance. For example, sexithiophene, one of the most widely studied oligomers, has been substituted at the β-positions of the thiophene ring system. This drastically improves the solubility but breaks the planarity of the π-system and more importantly its ability to pack in a structure where charge carriers can move freely.[7] In the few instances where the solubility barrier has been overcome, solution casting or spin coating has been used to fabricate devices, usually from halogenated solvents. Spin coating with oligomers and small molecules is very difficult because of their lower viscosity. Solution-cast films typically have an unpredictable morphology that is nonuniform and yield devices that vary greatly in terms of performance.[8] Recently, Afzali et al. demonstrated that high field effect mobility is obtainable with solution casting from a pentacene precursor.[9] The precursor is deposited by spin coating from halogenated solvents and then heated, which converts it into pentacene. In their work, there is no mention of the surface morphology or the variation in device performance. There are many factors in solution deposition that still need to be addressed such as surface free energy, aggregation dynamics, and surface crystallization. Nevertheless, the results are promising and competitive with that of vacuum deposition.

Since the ordering of multilayers is crucial to device performance, a rational choice for device fabrication is the layer-by-layer deposition technique. About 10 years ago, Decher and co-workers extended the pioneering work of Iler to a new preparative method for organized thin films.[10] It was demonstrated that multilayers could be prepared by alternatively dipping a substrate into solutions containing a positively and negatively charged polyelectrolyte. Exceptional film uniformity has been demonstrated with polyelectrolytes,[11] organic semiconductors,[12] and a variety of other functional molecules.[13] It has subsequently been used in an abundance of applications, some of which include thin film coatings, electro-optic devices,[14] biosensors,[15] catalysis,[16] nonlinear optics,[17] analytical separations,[18] and thin film dielectrics.[19] This technique is especially promising because of its simplicity and the ease in processability it offers.

It is generally believed that charge transport in organic molecules relies on weak electronic interactions between adjacent conjugated molecules. Therefore, good molecular ordering is extremely important in achieving high field effect mobility. Most organic semiconductors are unipolar, meaning they transport only one carrier type whether it is holes or electrons. Organic ambipolar transistors, having both n- and p-type behavior, have been reported in polymers containing ionic side chains,[20] and low-mobility blends.[21] Some applications, such as organic complementary circuits, require both p- and n-channel semiconductors and ambipolar materials could be used in their future design which eliminates the need to pattern p- and n-channel components separately.

In this study, we combine the properties of water-soluble phthalocyanine molecules and the ease of processability of the layer-by-layer deposition technique to fabricate air-stable, ambipolar FETs. To our knowledge, this is the first report of thin film transistors (TFTs) prepared using this technique. This system may also be used to answer some questions about the fabrication and mechanism of TFTs in general, such as the effect of polyelectrolytes, that is, electrostatic charges, water, and small ions, on device performance. In addition, it was previously reported that some ionic-containing species may undergo ion-assisted electrical conduction, which gives rise to ambipolar transistor behavior.[20] It is of interest to find out if the same effect is present in these phthalocyanine-containing thin films.

As stated above, many techniques have been developed to assemble phthalocyanines as thin films but the layer-by-layer control of composition and thickness is

(7) Bao, Z.; Zheng, J.; Bäuerle, P. Unpublished results.

(8) (a) Brown, A. R.; Pomp, A.; de Leeuw, D. M.; Klaassen, D. B. M.; Havinga, E. E.; Herwig, P.; Mullen, K. *J. Appl. Phys.* **1996**, *79* (4), 2136. (b) Garnier, F.; Hajlaoui, R.; Kassmi, A. E.; Horowitz, G.; Laigre, L.; Porzio, W.; Armanini, M.; Provasoli, F. *Chem. Mater.* **1998**, *10*, 3334. (c) Katz, H. E.; Li, W.; Lovinger, A. J.; Laquindanum, J. *Synth. Met.* **1999**, *102*, 897. (d) Hong, X. M.; Katz, H. E.; Lovinger, A. J.; Wang, B.-C.; Raghavachari, K. *Chem. Mater.* **2001**, *13*, 4686. (e) Laquindanum, J.; Katz, H. E.; Lovinger, A. J. *J. Am. Chem. Soc.* **1998**, *120*, 664.

(9) Afzali, A.; Dimitrakopoulos, C. D.; Breen, T. L. *J. Am. Chem. Soc.* **2002**, *124* (30), 8812.

(10) (a) Iler, R. K. *J. Colloid Interface Sci.* **1966**, *21*, 569. (b) Decher, G.; Hong, J.-D. *Makromol. Chem. Macromol. Symp.* **1991**, *46*, 321. (c) Decher, G.; Hong, J.-D. *Thin Solid Films* **1992**, *210−211*, 831. (d) Decher, G. *Science* **1997**, *277*, 1232.

(11) Lavalle, P.; Gergely, C.; Cuisinier, F. J. G.; Decher, G.; Schaaf, P.; Voegel, J. C.; Picart, C.; *Macromolecules* **2002**, *35* (11), 4458.

(12) (a) Cheung, J. H.; Stockton, W. B.; Rubner, M. F. *Macromolecules* **1997**, *30* (9), 2712. (b) Locklin, J.; Youk, J.-H.; Xia, C.; Park, M.-K.; Fan, X.; Advincula, R. *Langmuir* **2002**, *18* (3), 877. (c) Fan, X.; Locklin, J.; Youk, J.-H.; Blanton, W.; Xia, C.; Advincula, R. *Chem. Mater.* **2002**, *14* (5), 2184.

(13) (a) Caruso, F.; Furlong, D. N.; Ariga, K.; Ichinose, I.; Kunitake, T. *Langmuir* **1998**, *14* (16), 4559. (b) Liu, Y.; Wang, Y.; Lu, H.; Claus, R. O. *J. Phys. Chem. B.* **1999**, *103* (12), 2035.

(14) (a) Fou, A. C.; Onitsuka, O.; Ferreira, M.; Rubner, M. F.; Hsieh, B. R. *J. Appl. Phys.* **1996**, *79*, 7501. (b) Wu, A.; Yoo, D.; Lee, J. K.; Rubner, M. F. *J. Am. Chem. Soc.* **1999**, *121*, 4883.

(15) (a) Decher, G.; Lehr, B.; Lowack, K.; Lvov, Y.; Schmitt, J. *Biosens. Bioelectron.* **1994**, *9*, 677. (b) Caruso, F.; Furlong, D. N.; Ariga, K.; Ichinose, I.; Kunitake, T. *Langmuir* **1998**, *14*, 4559.

(16) Onda, M.; Ariga, K.; Kunitake, T. *J. Biosci. Bioeng.* **1999**, *87*, 69.

(17) Herman, W. N.; Wynne, K. J. *J. Am. Chem. Soc.* **1998**, *120*, 11202.

(18) Graul, T. W.; Schlenoff, J. B. *Anal. Chem.* **1999**, *71*, 4007.

(19) Durstock, M. F.; Rubner, M. F. *Langmuir* **2001**, *17*, 7865.

(20) Chen, X. L.; Bao, Z.; Schon, J. H.; Lovinger, A. J.; Lin, Y.-Y.; Crone, B.; Dodabalapur, A.; Batlogg, B. *Appl. Phys. Lett.* **2001**, *78 (2)*, 228.

(21) (a) Tada, K.; Harada, H.; Yoshino, K. *Jpn. J. Appl. Phys., Part 2* **1996**, *35*, L944. (b) Tada, H.; Touda, H.; Takada, M.; Matsushige, K. *Appl. Phys. Lett.* **2000**, *76*, 873.

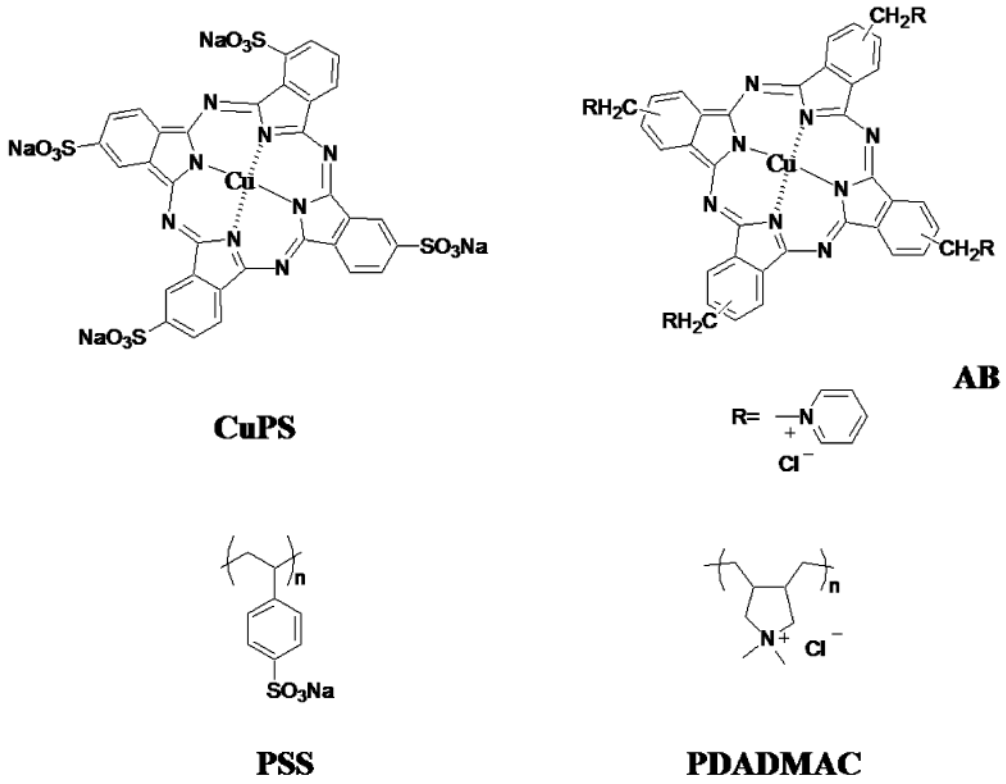

Figure 1. Chemical structure of the materials used in thin film fabrication.

still a challenge. Thermal evaporation is the most widely used technique, but this is limited to volatile, thermally durable materials. Cooper et al. demonstrated the applicability of the layer-by-layer deposition process to phthalocyanines with their incorporation into polypeptide-dye multilayers.[22] As for the order of the phthalocyanine molecules in the multilayers, they observed dimer formation based on the changes in the Q-band absorption spectrum with no evidence of higher aggregates in any of their films.

Electrostatic attraction between the charged substrate and adsorbed molecule is the energetic driving force for multilayer formation. However, it is increasingly complicated to describe the molecular packing arrangement of the material based on electrostatics alone. Most likely, this is determined by competition between hydrophobic effects, electrostatics, and many other factors. Also, it is unclear whether the molecules are adsorbed as small aggregates from solution or as larger micelles. Therefore, it is of great interest to gain more insight into the adsorption process and the factors affecting molecular orientation, which can considerably affect the carrier mobility in traditional organic FETs. Here, we report the fabrication of phthalocyanine-based field effect transistors from aqueous and 0.03 M NaCl solutions that operate under ambient conditions where ion-modulated electrical conduction was found to be the conduction mechanism.

Experimental Section

Materials. All essential chemicals and reagents were purchased from Aldrich. Alcian blue-tetrakis(methyl pyridinium) chloride (AB) and copper(II) phthalocyanine-3,4′,4″,4‴-tetrasulfonic acid, tetrasodium salt (CuPS) were rinsed with acetone prior to use. Poly(sodium 4-styrenesulfonate) (PSS; MW ca. 70000) and poly(diallyldimethylammonium chloride) (PDADMAC; MW ca. 100000−200000) were used without further purification. Their chemical structures are shown in Figure 1.

Multilayer Preparation. Ultrapure water was used for all experiments and all cleaning steps, which was obtained by an ion-exchange and filtration unit (Milli-Q Academic, Millipore Corp.). The resistivity was 18.2 MΩ·cm. Silicon wafers and glass microscope slides were cut into pieces 2.5 × 3.0 cm^2. The substrates were rigorously sonicated with Fisher sonicating solution, water, 2-propanol, and acetone for 15−20 min each. This was followed with plasma cleaning (Plassmod March Instruments Inc.) in an argon atmosphere for 6 min. They were then soaked in piranha solution (30% H_2O_2/70% H_2SO_4 v/v) for 30 min (*Caution*: piranha is a strong oxidizer that should be handled with care and not stored in closed containers) and thoroughly rinsed by sonication in water. They were then dried completely and submerged into freshly distilled toluene containing 0.5 wt % of 3-aminopropyltriethoxysilane (APS) for functionalization. After 30 min, the solution was discarded and toluene was added and sonicated for 15 min. Half of the toluene was then discarded, acetone added, and the container sonicated for an additional 10 min. Finally, the substrates were sonicated in acetone for 10 min, dried, and stored in 0.01 M HCl solution overnight. The APS layer thickness was 10.0 Å as determined by ellipsometry. Water contact angle measurements (Model CAM-Micro, Tantec Inc.) were taken before and after functionalization to ensure silanization by monitoring the change in hydrophilicity of the surface for the glass substrates.

Prior to deposition of AB or CuPS, three layers of polyelectrolyte (PSS/PDADMAC/PSS) were deposited to ensure an evenly charged surface and increase the surface charge density of the substrate (see Transistor Measurements section). The concentration of polymer solutions was 1 mg/mL in pure H_2O. AB and CuPS solutions (0.5 mg/mL) in water and 0.03 M NaCl were also prepared. Multilayers were then built up by alternating deposition of AB and CuPS until the desired layer number was reached. This was either done by hand or with

(22) Cooper, T. M.; Campbell, A. L.; Crane, R. L. *Langmuir* **1995**, *11*, 2713.

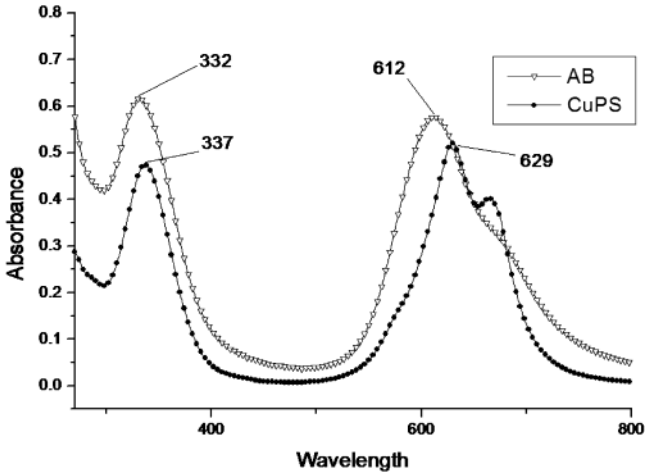

Figure 2. UV−vis absorption spectra in solution: (a) AB and (b) CuPS in water.

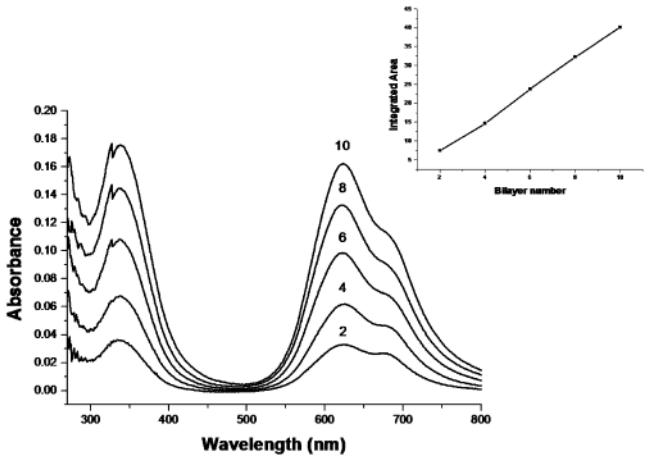

Figure 3. UV−vis absorbance spectra of multilayer films (1−10 bilayers) prepared from 0.03 M NaCl solution. The inset shows the integrated area under the peaks vs bilayer number.

the aid of an automated dipping machine (HMS Series Programmable Slide Stainer, Carl Zeiss, Inc.). A dipping period of 30 min was used for AB and CuPS, with rinsing, drying, and measurements taken in between.

Measurements. The UV−vis spectra were obtained with a Perkin-Elmer spectrophotometer (Lambda 20) using a quartz cuvette or glass slide. Polarization UV−vis absorption measurements were performed at normal and oblique incidence to investigate the in-plane and out-of-plane anisotropy. Ellipsometric thickness measurements were performed on a Multiskop (Optrel GbR) with a 632.8-nm He−Ne laser beam as the light source. Five measurements were taken for each layer and the results were averaged. Delta and psi values were measured and thickness data were calculated by integrated specialized software (Multi, Optrel GbR) using $n = 1.6$ and $k = 0.1$ for the phthalocyanine layers.

Atomic force microscopic (AFM) images were taken in air by the PicoScan system (Molecular Imaging) equipped with a 7×7 μm scanner. Magnetic AC (MAC) mode (a noncontact mode) was used for all of the images. A MAC lever, a silicon nitride-based cantilever coated with magnetic film, was used as an AFM tip. The force constant of the tip was 0.5 N/m and the resonant frequency was around 100 kHz. All samples were measured inside a suspension chamber to minimize ambient disturbance.

Current−voltage characteristics were obtained with a Hewlett-Packard (HP) 4155A semiconductor parameter analyzer. Both top and bottom contact geometries were used for measurements. The Si substrate is n-doped with an oxide layer of 300 nm as the gate dielectric with a capacitance per unit area of 10 nF/cm^2. For the bottom contact geometry, gold electrodes forming channels of 250-μm width *(W)* and 1.5−25-μm length *(L)* were photolithographically defined. The AB/CuPS layers were then deposited over the entire electrode/dielectric surface. For the top contact geometry, gold electrodes were defined after the layer-by-layer deposition by using shadow masks with a $(W/L) = 5.5$. The measurements were carried out under ambient conditions unless otherwise indicated.

Results and Discussion

UV−Vis Spectrometry. Parts (a) and (b) of Figure 2 show the UV−vis absorption spectra of AB and CuPS, respectively. The absorbance band in the UV, termed the Soret band, occurs around 332 and 337 nm for AB and CuPS, respectively. This band is responsible for the deep blue color of the materials. The Q-band, occurring at 612 and 629 nm for AB and CuPS, respectively, is also typical of phthalocyanine materials. The band edge has been assigned to a $\pi-\pi^*$ transition from the highest occupied molecular orbital (HOMO) to the lowest unoccupied molecular orbital (LUMO) through extended Hückel calculations by Schaffer et al.[23] The position of the Q-band is more sensitive to substitution and environment than the Soret band in most cases.

Multilayer Growth. The formation of multilayer assemblies of AB and CuPS on the various substrates proceeded in a linear and stepwise fashion. The substrates were pre-deposited with three layers of polyelectrolyte prior to deposition of AB to ensure maximum surface charge density and to provide equal surface conditions within each type of substrate. The multilayer growth was monitored by UV−vis absorption spectroscopy and ellipsometry thickness measurements were taken between each layer. Figure 3 shows the UV−vis absorption spectra of the film prepared from 0.03 M NaCl. The intensity of absorbance increases linearly with the number of dipping cycles, indicating a stepwise and regular growth process. The inset of Figure 3 plots the integrated area under each bilayer to verify the linear increase with each layer number. Also, the position of the Q-band does not change much with respect to the solution, indicating a small amount, if any, higher aggregate formation upon adsorption.

Figure 4 shows the thickness increase for the thin films measured by ellipsometry. There is a linear, stepwise increase in thickness with increasing layer number that is consistent with the orderly increase in absorption intensity as shown by UV−vis. The average bilayer thickness is 10.5 Å for AB/CuPS in pure H_2O and 15.6 Å from 0.03 M NaCl. The total film thickness is 111.5 Å from pure H_2O and 170.0 Å from 0.03 M NaCl after 10 bilayers. These thickness results are similar to those reported by Li et al. for nickel phthalocyanine, sulfonated salt, and polyelectrolyte multilayers in which X-ray reflectometry was used in addition to ellipsometric measurements.[24] However, it is evident that the presence of salt increased the average thickness per layer but with reduced linearity. This has been consistently observed with other layer-by-layer systems where salts play an important role in the aggregation process and the layer packing arrangement.[12c,25]

(23) Schaffer, A. M.; Gouterman, M.; Davidson, E. *Theor. Chim. Acta* **1973**, *30*, 9.

(24) (a) Li, D.; Lutt, M.; Fitzsimmons, M. R.; Synowicki, R.; Hawley, M. E.; Brown, G. W. *J. Am. Chem. Soc.* **1998**, *120*, 8797. (b) Lutt, M.; Fitzsimmons, M. R.; Li, D. *J. Phys. Chem. B* **1998**, *102*, 400.

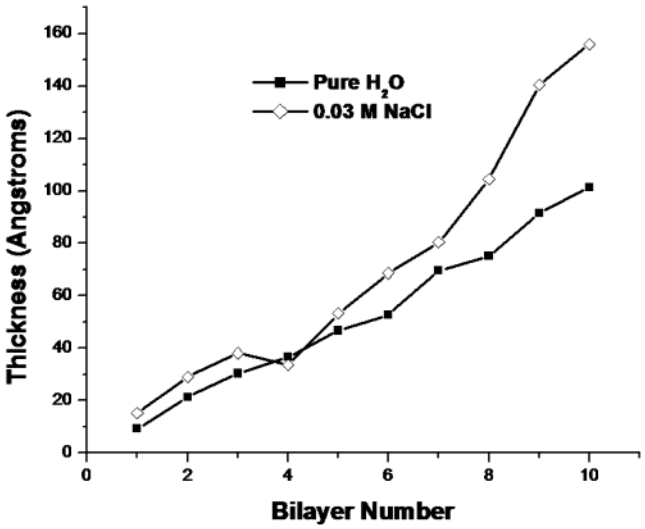

Figure 4. Thickness increase of AB/CuPS multilayers with increasing layer number determined by ellipsometry.

The molecular orientation of the phthalocyanine molecules in the solid state is of great interest because it is thought to strongly affect the carrier mobility in electronic devices, such as FETs and photovoltaic cells. The UV−vis absorption of the $\pi-\pi^*$ transition is very sensitive to the direction of polarization of incident light and has proven to be a useful tool for the analysis of the structural anisotropy of thin films.[26] Parts (a) and (b) of Figure 5 show the polarized UV−vis absorbance spectra of 10 bilayers of AB/CuPS prepared from 0.03 M NaCl at a 90° and 45° incidence angle, respectively. The electric field is parallel (p-polarization) and perpendicular (s-polarization) to the plane of the substrate as shown in the figure insert. At 90°, the shape and position of the absorption bands does not change according to the polarization mode. In the case of the spectra recorded at a 45° incidence angle, either with the electric field in the plane of the substrate (s-polarization) or perpendicular to the plane (p-polarization), stronger absorption intensities are obtained from the s-polarization mode. From these two experimental geometries, it can be concluded that the $\pi-\pi^*$ absorption of the phthalocyanine molecules exhibits a polarization dependence. Since no change in absorption intensity is observed in the case of 90° and a large difference is observed at 45° with the s-component being greater, it can be concluded that the phthalocyanine molecules lie relatively flat with respect to the substrate surface. It also tells us that the phthalocyanine molecules have a random orientation within the plane of the substrate, which is to be expected since there is no preferred dipping direction as adsorption occurs.

Transistor Measurements. The field effect transistor is a three-terminal device in which the current flow through two terminals is controlled by a voltage at the third. Its basic structure is shown in Figure 6. The FET is comprised of the following components: electrodes (the source, drain, and gate), a dielectric layer, and a semiconducting layer. The current flow between the drain and source electrodes (I_{DS}) is modulated by the applied gate voltage (V_G). An "off state" of the transistor is when no gate voltage is applied between the drain and source electrodes ($V_G = 0$). I_{DS} is usually very low in the off state as long as the semiconducting material is not highly doped. When a voltage is applied at the gate, charges are induced into the semiconducting layer at the interface between the semiconductor and dielectric layer. As a result, the drain-source current increases due to the increased number of charge carriers. This is the "on state" of the transistor. For p-channel devices, holes are the major charge carriers whereas electrons are the major charge carriers for n-channel transistors. Recent reviews on organic FETs can be found elsewhere.[27]

Transistors were fabricated under a variety of conditions and the field effect mobilities of each device type are shown in Table 1. To show the precision of each measurement, the data are reported as a range where at least 10 devices were tested for each deposition condition. Parts (a) and (b) of Figure 7 show the typical $I_{DS}-V_{DS}$ plot for the layer-by-layer transistors operating at different gate voltages at both negative and positive gate biases, respectively. When a negative (or positive) bias is applied, the drain-source current scales with the negative (or positive) gate voltage.

For purposes of comparison with other organic FETs, the mobilities have been calculated by standard field effect transistor equations. Since the shape of the graph and mechanism of charge propagation may be different in these "ambipolar" transistors, the mobilities calculated are just estimations and by no means an absolute value. In traditional metal−insulator−semiconductor field effect transistors (MISFETs), there is typically a linear and saturated regime in the I_{DS} vs V_{DS} curve at various V_G. At low V_{DS}, I_{DS} increases linearly with V_{DS} and can be approximated by

$$I_{DS} = \frac{WC_i}{L}\mu\left(V_G - V_T - \frac{V_{DS}}{2}\right)V_{DS}$$

where W is the channel width, L is the channel length, C_i is the capacitance per unit area of the insulating layer, V_T is the threshold voltage, and μ is the field effect mobility. From this equation, the mobility can be calculated in the linear regime from the transconductance

$$g_m = \left(\frac{\partial I_{DS}}{\partial V_G}\right)_{V_{DS}=\text{const}} = \frac{WC_i}{L}\mu V_{DS}$$

by plotting I_{DS} vs V_G at a constant V_{DS} and equating the value of the slope of this plot to the transconductance.

Also, μ may be calculated by determining the slope $[(\partial I_{DS}/\partial V_{DS})_{V_{G=\text{const}}}]$ in the linear regime of the I_{DS} vs V_{DS} curve at various V_G. These slopes are then plotted

(25) (a) Clark, S. L.; Montague, M. F.; Hammond, P. T. *Macromolecules* **1997**, *30*, 7237. (b) Hong, J.-D.; Park, E.-S.; Park, A.-L. *Langmuir* **1999**, *15*, 6515. (c) McAloney, R. A.; Sinyor, M.; Dudnik, V.; Goh, M. C. *Langmuir* **2001**, *17*, 6655.

(26) (a) Rikukawa, M.; Rubner, M. F. *Langmuir* **1994**, *10*, 519. (b) Xu, G.; Bao, Z.; Groves, T. *Langmuir* **2000**, *16*, 1834. (c) Zhang, Z.; Verma, A. L.; Yoneyama, M.; Nakashima, K.; Iriyama, K.; Ozaki, Y. *Langmuir* **1997**, *13*, 4422. (d) Bolognesi, A.; Bertini, F.; Bajo, G.; Provasoli, A.; Villa, D.; Ahumada, O. *Thin Solid Films* **1996**, *289*, 129.

(27) (a) Lovinger, A. J.; Rothberg, L. J. *J. Mater. Res.* **1996**, *11*, 1581. (b) Horowitz, G. *J. Mater. Chem.* **1999**, *9*, 2021. (c) Katz, H. E.; Bao, Z. *J. Phys. Chem. B* **2000**, *104*, 671.

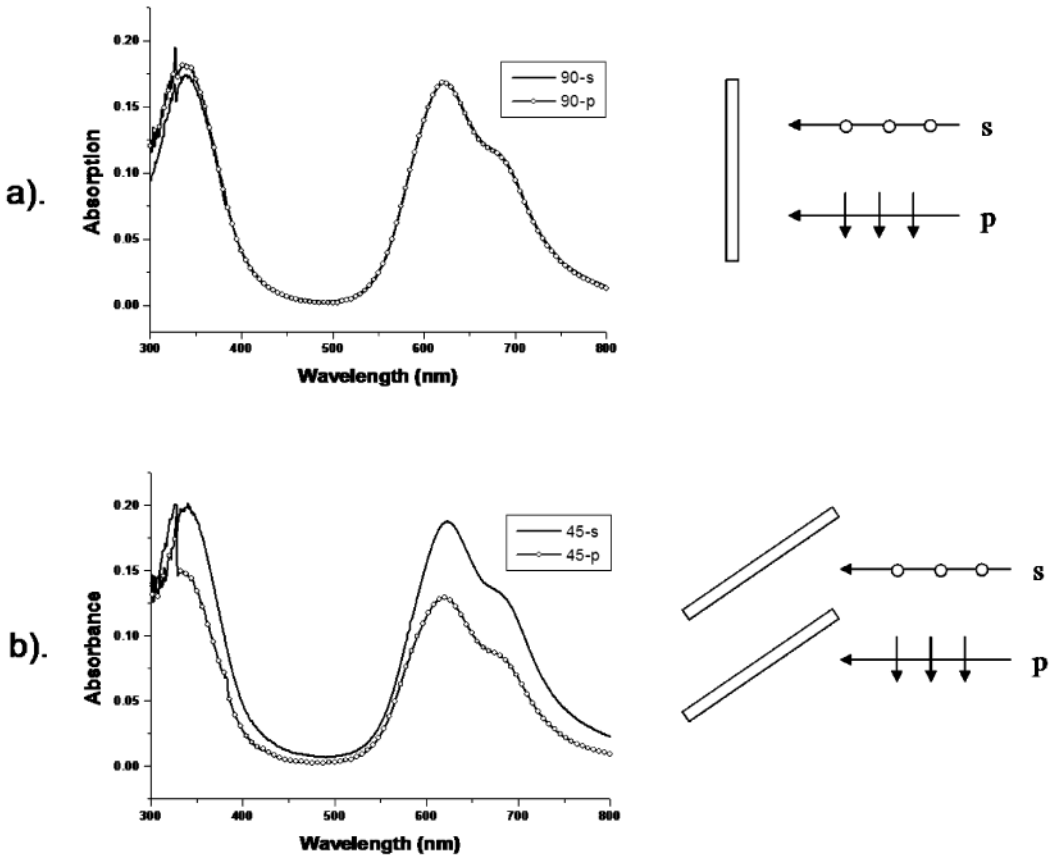

Figure 5. Polarized UV−vis absorption spectra of AB/CuPS of 10 bilayers prepared from 0.03 M NaCl solution at (a) 90° and (b) 45°.

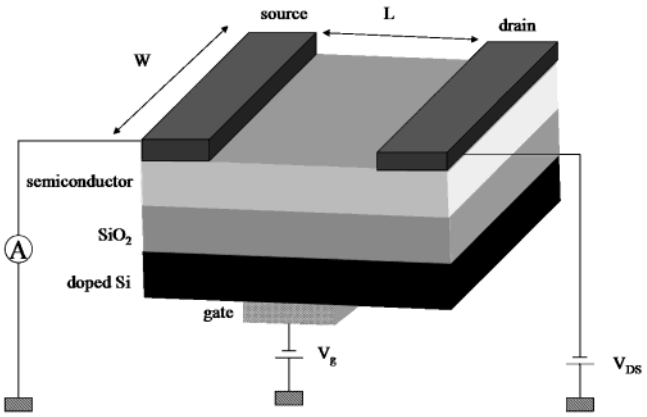

Figure 6. Schematic diagram showing the basic components of organic field effect transistors in the top contact geometry. The alternative bottom contact geometry has the source and drain electrode on the semiconductor-dielectric interface.

vs V_G, and the slope of this plot $(\partial/\partial V_G)$ $[(\partial I_{DS}/\partial V_{DS})_{V_{G=const}}]_{V_{DS=const}}$ is equal to $(WC_i/L)\mu$.

In the saturated regime, μ can be approximated by the slope of the plot of $|I_{DS}^{1/2}|$ vs V_G.[28] In all of our devices prepared under different conditions, the mobility values calculated from the linear regime are higher by a factor of 2 or greater than those calculated using this approximation.

The shape of the graphs in (a) and (b) of Figure 7 are unusual for organic transistors in that the current does not saturate with increasing applied gate voltage. It increases almost linearly with increasing V_{DS} at a given gate bias, indicating an electric-field-dependent charge density or mobility. Also, the entire set of $I-V$ curves shift up when there is no time delay between repeated scans. After about 15−30 s, the $I-V$ curves return to their original positions or values. The devices can be operated in air for long periods of time with very reproducible $I-V$ curves. The device shown in Figure 7 is one of at least 10 devices on the same wafer that produced similar results. The off-current in these phthalocyanine devices are relatively high (∼200 nA for the devices shown) whereas those made from vacuum-sublimed phthalocyanines are usually on the order of pA or a few nA. This high off-current behavior may be related to contributions from ionic currents to mobile ions introduced during the layer-by-layer deposition process.

Table 1 also shows the variation of mobility with different gap sizes (distance between the source and drain electrodes) in the bottom contact device geometry. As the gap size is increased, the mobility decreases. At smaller gap sizes (1.5 μm), there is a large increase in current but the gate effect is lost. This also indicates an electric-field-dependent mobility where ionic conductivity plays a role when the electrodes are separated by a smaller gap.

Similar ambipolar behavior has been reported for certain conducting polymers containing ionic side chains.[20,29] In our case, the ambipolar nature of the multilayers can be related to the amount of mobile ions in the film. Polyelectrolyte multilayers have been known

(28) Dimitrakopoulos, C. D.; Brown, A. R.; Pomp, A. *J. Appl. Phys.* **1996**, *80 (4)*, 2501.

(29) Babel, A.; Jenehke, S. A. *Adv. Mater.* **2002**, *14*, 371.

Table 1. Field Effect Mobilities of Devices Fabricated under Various Conditions[a]

AB/CuPS multilayers deposited under various conditions	mobility, (μ) in (cm^2/V·s) calculated from saturated approximation.	mobility, (μ) in (cm^2/V·s) calculated from the multiple V_G's	mobility, (μ) in (cm^2/V·s) calculated from the transconductance
pure H_2O (top contact, 40-μm gap, $W/L = 5.5$)	(p) 1.41×10^{-5} to 1.46×10^{-5} (n) 4.40×10^{-6} to 5.20×10^{-6}	(p) 3.31×10^{-5} to 3.52×10^{-5} (n) 1.88×10^{-5} to 2.03×10^{-5}	(p) 2.58×10^{-5} to 2.91×10^{-5} (n) 1.36×10^{-5} to 1.38×10^{-5}
0.03 M NaCl (top contact, 40-μm gap, $W/L = 5.5$)	(p) 7.51×10^{-5} to 9.31×10^{-5} (n) 7.10×10^{-5} to 1.04×10^{-4}	(p) 1.68×10^{-4} to 2.06×10^{-4} (n) 1.94×10^{-4} to 2.02×10^{-4}	(p) 1.55×10^{-4} to 2.32×10^{-4} (n) 1.72×10^{-4} to 2.02×10^{-4}
0.03 M NaCl without PE prelayers (top contact, 40-μm gap, $W/L = 5.5$)	(p) 4.07×10^{-5} to 1.45×10^{-4} (n) 7.30×10^{-5} to 1.15×10^{-4}	(p) 6.94×10^{-5} to 2.44×10^{-4} (n) 2.23×10^{-4} to 2.33×10^{-4}	(p) 6.96×10^{-5} to 2.33×10^{-4} (n) 2.27×10^{-4} to 2.6×10^{-4}
pure H_2O (bottom contact, 15-μm gap, $W/L = 17$)	(p) 2.62×10^{-5} to 3.43×10^{-5} (n) 2.04×10^{-5} to 3.12×10^{-5}	(p) 7.44×10^{-5} to 9.09×10^{-4} (n) 8.01×10^{-5} to 8.51×10^{-5}	(p) 7.05×10^{-5} to 1.11×10^{-4} (n) 8.91×10^{-5} to 1.06×10^{-4}
0.03 M NaCl (bottom contact, 15-μm gap, $W/L = 17$)	(p) 1.60×10^{-4} to 2.32×10^{-4} (n) 1.11×10^{-4} to 1.13×10^{-4}	(p) 3.54×10^{-4} to 3.80×10^{-4} (n) 2.37×10^{-4} to 2.55×10^{-4}	(p) 3.37×10^{-4} to 3.54×10^{-4} (n) 2.22×10^{-4} to 2.55×10^{-4}
0.03 M NaCl (bottom contact, 27-μm gap, $W/L = 9.44$)	(p) 6.40×10^{-5} to 8.45×10^{-5} (n) 4.91×10^{-5} to 8.25×10^{-5}	(p) 1.12×10^{-4} to 1.60×10^{-4} (n) 1.34×10^{-4} to 1.55×10^{-4}	(p) 8.77×10^{-5} to 1.80×10^{-4} (n) 1.46×10^{-4} to 1.48×10^{-4}

[a] Values are reported as a range where at least ten different transistors were tested for each condition. (p) and (n) represent the p-channel and n-channel device conditions, respectively.

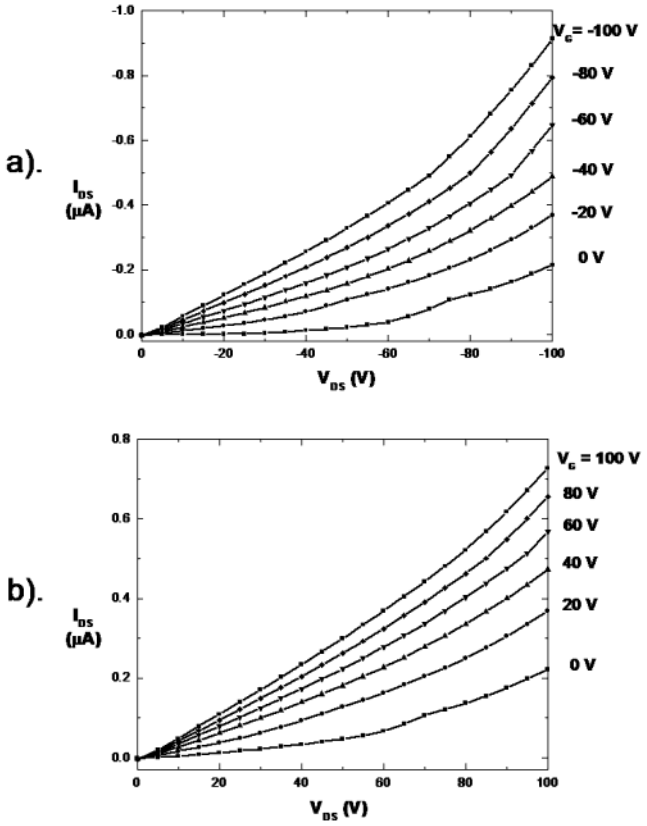

Figure 7. Typical I_{DS} vs V_{DS} curves at (a) negative and (b) positive gate bias for the AB/CuPS multilayers fabricated from 0.03 M NaCl solution with a gap of 14 μm.

to incorporate around 20 wt % water,[30] which provides a medium for mobile ions in the transistors. When the devices were dried under vacuum (10^{-3} Torr) for 24 h and most of the water was removed, both p- and n-type behavior ceased. This is likely since the geometry of the phthalocyanine molecules in the film is such that minimal $\pi-\pi$ stacking can occur. The ambipolar behavior can be recovered upon re-exposure to ambient conditions.

To see if there was any effect on the mobility due to the polyelectrolyte prelayers, films were prepared without PDADMAC and PSS at the beginning of the dipping cycles. The mobilities are also shown in Table 1. The deposition also proceeded in a similar fashion, but after a considerable number of deposition cycles, there were visible patches of material and some places where deposition did not occur on the film. This was due to the decreased charge density of the surface provided by the self-assembled monolayer (SAM) of APS.

In layer-by-layer deposition, it is well-known that any surface charge defects in the monolayer can be overcompensated by using polyelectrolytes prior to deposition of small molecules. Polyelectrolytes, with their large number of ionic groups, can bridge the underlying defects in the SAM.[10d,31] In this sense, the surface morphology and charge density at the semiconductor−insulator interface is dominated by the polyelectrolyte layers and not the substrate or the SAM. Using a polyelectrolyte-modified SiO_2 surface does bring about changes in the performance of the devices, but not to the extent that it does with other vacuum-deposited organic semiconductors where ions do not play an important role in the device.

To see the effect of polyelectrolytes on the transistor performance of a typical organic semiconductor, pentacene films were vacuum-deposited at room temperature on untreated and polyelectrolyte-treated wafers. The mobility (calculated from the saturated region) was significantly decreased in the case of the treated wafers (bare SiO_2, $\mu = 0.25$ cm^2/V·s; polyelectrolyte, $\mu = 0.02$ cm^2/V·s), which can be partially attributed to the sizes of the grains of organic material deposited on the substrate surface. Figure 8 shows the AFM images of the vacuum-deposited pentacene films at room temperature on bare SiO_2 (left) and the polyelectrolyte-modified surface (right). It is difficult to say for certain if this change in grain size is due to the morphological change at the surface or the introduction of ionic groups but it is a significant change nonetheless.

In the past, TGA,[18] XPS,[12b,32] neutron reflectometry,[33] and radioanalytical techniques[34] have been used to detect the presence of small ions in films fabricated by layer-by-layer adsorption and in most cases have failed to detect their presence. These results seem to indicate

(30) Farhat, T.; Yassin, G.; Dubas, S.; Schlenoff, J. *Langmuir* **1999**, *15*, 6621.
(31) Laschewsky, A. *Eur. Chem. Chron.* **1997**, *2*, 13.
(32) Laurent, D.; Schlenoff, J. B. *Langmuir* **1997**, *13*, 1552.
(33) Schmitt, J.; Grunewald, T.; Decher, G.; Pershan, P. S.; Kjaer, K.; Losche, M. *Macromolecules* **1993**, *26*, 7058.
(34) Schlenoff, J. B.; Li, M. *Ber. Bunsen-Ges. Phys. Chem.* **1996**, *100*, 943.

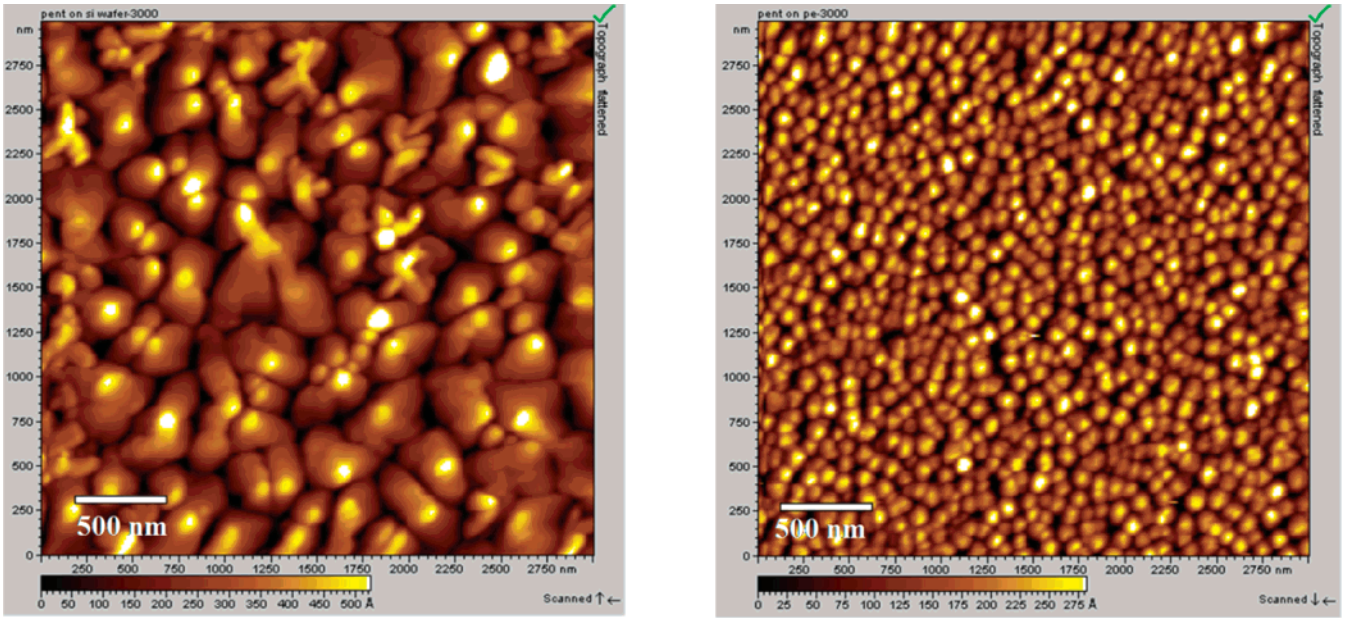

Figure 8. $3 \times 3\ \mu$m AFM images of vacuum-deposited pentacene at room temperature onto bare SiO_2 (left) and a polyelectrolyte-treated SiO_2 surface (right). The scale bar shown is 500 nm.

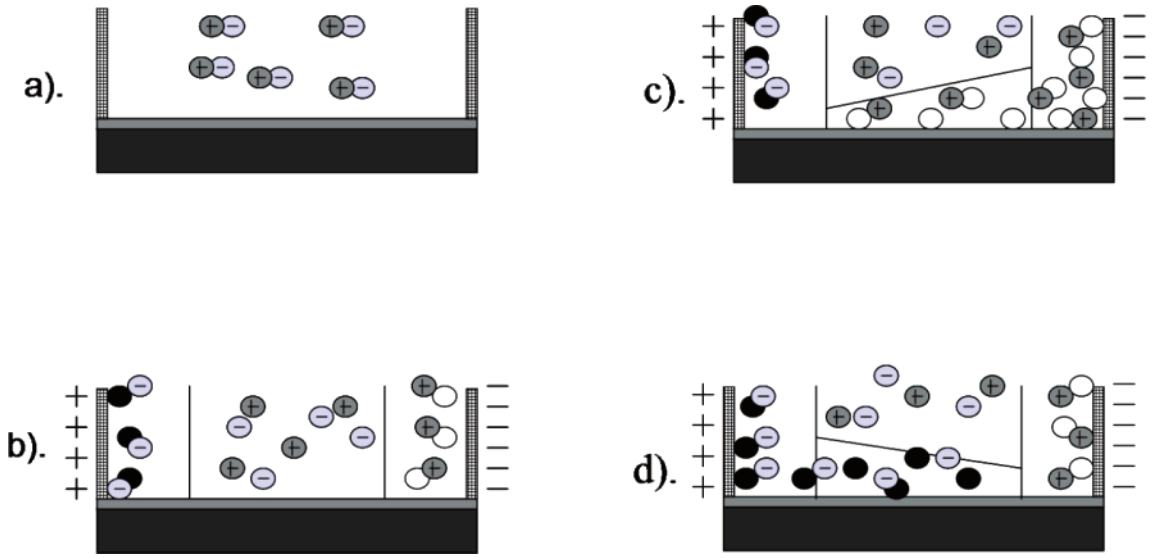

Figure 9. Schematic diagram of the proposed ambipolar transistor mechanism: (a) idle state; (b) off state, (c) on state for n-type, and (d) on state for p-type (○ reduced molecules, ● oxidized molecules, ⊕ cations from ionic species, ⊖ anions from ionic species).

that the amount of small ions incorporated into the film is minimal. One especially interesting example is from Durstock and Rubner, where changes in the dielectric behavior and conductivity of multilayer films made of polyelectrolytes were monitored under different temperatures and conditions.[19] They were able to qualitatively show that more small ions are incorporated into films that included added salt in the solutions during the dipping cycles than were from pure water. Our results also indicate that the same is true for the layer-by-layer deposition of small molecules. There is an increase in the field effect mobility for the films deposited from saline solution, indicating that more small ions are incorporated into the films than that of the pure water system.

Transistor Mechanism. On the basis of these observations, we propose that the multilayers undergo ion-assisted electrochemical doping during transistor operation similar to that reported by Chen et al. for certain polymers containing ionic side chains.[20] The phthalocyanine molecules at the semiconductor−electrode interface are oxidized or reduced during charge injection. Charge transport is realized by a hopping mechanism of holes or electrons from one molecule to another throughout the film. The mobile ions present in the film migrate to the channel region of the transistor and act to balance and stabilize the charge of the electrically doped small molecules. The proposed mechanism is schematically shown in Figure 9. In the idle state of the transistor, the ions are electrostatically bound to each other and all charges are compensated for. In the off state, some of the ions are used to stabilize an amount of the radical cations and anions produced by the applied bias (V_{DS}) at the electrode−semiconductor interface. When a gate bias is applied (V_G), the ions help to stabilize the holes or electrons at the semiconductor−insulator interface, providing a larger channel where charges can propagate. Both the polarity and the extent

of doping are modulated by the applied V_G. The current we observed should be due to electronic conduction instead of ionic conduction since the current stabilizes at a given drain source and gate voltage where an ionic current will decrease with time.

Conclusions

AB/CuPS alternating multilayers were successfully prepared from both pure water and 0.03 M NaCl solution using the layer-by-layer deposition technique. The multilayer growth proceeded in a stepwise and regular fashion. Our results indicate that the phthalocyanine molecules lie relatively flat with respect to the substrate surface and have a random orientation within the plane of the substrate. Field effect transistors were successfully fabricated from the multilayers, which showed unusual "ambipolar" transistor-like behavior. The operating mechanism involves ion-assisted electrochemical doping and the magnitude of the field effect mobility was found to rely on the amount of small ions available in the film. Further investigation is underway with regard to adsorption behavior of other phthalocyanine molecules and their possible use as FET sensors.

Acknowledgment. The authors would like to thank Edwin Chandross, Bert De Boer, Chuanjun Xia, Xiaowu Fan, and Derek Patton for helpful discussions. Funding from the U.S. Department of Education through a Graduate Assistance in Areas of National Need (GAANN) Grant P200A0009000 (J.L.), Lucent Technologies Summer Internship (J.L.), and NSF Career Grant DMR-9982010 are greatly appreciated.

CM021073F